Title

The Effects of Adipose-Derived Stem Cells Differentiated Into Endothelial Cells and Osteoblasts on Healing of Critical Size Calvarial Defects.

Journal

The Journal of craniofacial surgery, 28(7)

ISSN

1049-2275

Authors

Orbay, Hakan
Busse, Brittany
Leach, Jonathan Kent
et al.

Publication Date

2017-10-01

DOI

10.1097/scs.0000000000003910

Peer reviewed

The Effects of Adipose-Derived Stem Cells Differentiated Into Endothelial Cells and Osteoblasts on Healing of Critical Size Calvarial Defects

Hakan Orbay, MD, PhD, Brittany Busse, MD,* Jonathan Kent Leach, PhD,†‡ and David E. Sahar, MD, FACS**

Abstract: Delayed vascularization and resultant resorption limits the clinical use of tissue engineered bony constructs. The objective of this study is to develop a strategy to accelerate the neovascularization of tissue-engineered bony constructs using endothelial differentiated adipose-derived stem cells (ASC). The authors harvested ASC from inguinal fat pads of male Lewis rats (n = 5) and induced toward endothelial and osteoblastic lineages. The authors created critical size calvarial defects on male Lewis rats (n = 30) and randomized the animals into 4 groups. For the repair of the defects the authors used hydroxyapatite/poly(lactide-co-glycolide) [HA-PLG] scaffolds in group I, HA-PLG scaffolds seeded with ASC in group II, HA-PLG scaffolds seeded with ASC-derived endothelial cells in group III, and HA-PLG scaffolds seeded with ASC-derived osteoblasts in group IV. The authors evaluated the bone healing histologically and with micro-computed tomography (CT) scans 8 weeks later. Adipose-derived stem cells exhibited the characteristics of endothelial and osteogenic lineages, and attached on HA-PLG scaffolds after differentiation. Micro-CT analysis revealed that highest bone mineral density was in group IV (1.46 ± 0.01 g/cm^3) followed by groups III (1.43 ± 0.05 g/cm^3), I (1.42 ± 0.05 g/cm^3), and II (1.3 ± 0.1 g/cm^3). Hematoxylin–Eosin and Masson Trichrome staining revealed similar results with the highest bone regeneration in group IV followed by groups II, III, and I. Regenerated bone in group IV also had the highest vascular density, but none of these differences achieved statistical significance ($P > 0.05$). The ASC-derived endothelial cells and osteoblasts provide a limited increase in calvarial bone healing when combined with HA-PLG scaffolds.

Key Words: Bone, multipotent, regeneration, skull, stem cells

(*J Craniofac Surg* 2017;28: 1874–1879)

Large bony defects usually exceed the physiologic regenerative capability of human body and require bone grafts or biomaterials for adequate healing.[1,2] These approaches are in large part successful but they come with inherent disadvantages. The use of bone grafts is limited by donor-site morbidity, resorption, and additional operative risk, whereas biomaterials are prone to exposure and infection.[1,3,4] In addition, the survival of bone grafts may be impaired by previous irradiation, contamination, and compromised vascularity in the recipient bed.

Tissue engineering uses scaffolds, signals, and cells to synthesize tissues in vitro, offering an exciting solution to problems faced with traditional bone substitutes.[2,3,5] An ideal bone substitute, which is inert, inexpensive, structurally fortified, and fully osteoconductive, can be obtained using tissue engineering methods.[3] However, angiogenesis and neovascularization are critical processes in bone regeneration and the success of bone tissue engineering is hampered by the lack of an efficient blood circulation within the bony scaffolds. A variety of approaches have been applied to promote the vascularization of bony scaffolds including the localized delivery of potent proangiogenic macromolecules.[6–8] Coseeding of endothelial cells and mesenchymal stem cells on osteogenic scaffolds were also shown to promote vascularization and bone regeneration.[9,10] Endothelial cells can be a viable alternative to costly macromolecules; however, due to the associated donor site morbidity and limited proliferation capacity, the clinical use of mature endothelial cells can be challenging.[11] Adipose-derived stem cells (ASC) differentiate into both endothelial and osteogenic lineages.[12–14] With abundant donor tissue and ease of harvest, ASC can serve as a source of endothelial cells and osteoblasts for bone tissue engineering.

Adipose-derived stem cells secrete a number of trophic factors, can prime the local microenvironment and stimulate angiogenesis within the scaffolds,[15,16] but it is unlikely that the ASC will spontaneously differentiate into osteoblasts and endothelial cells in vivo after transplantation due to the lack of external cues.[17] Therefore, differentiation of ASC into osteogenic and endothelial lineages in vitro (before transplantation) represents a more effective strategy for bone regeneration. The differentiated cells have the potential to stimulate osteogenesis and neovascularization, and enable a more complete reconstructive effort.

In this study, we combined a resorbable hydroxyapatite/poly(lactide-co-glycolide) [HA-PLG] scaffold and ASC-derived

From the *Department of Surgery, University of California—Davis Medical Center, Sacramento; †Department of Biomedical Engineering, University of California—Davis, Davis; and ‡Department of Orthopedic Surgery, University of California—Davis Medical Center, Sacramento, CA.

Received March 10, 2017.
Accepted for publication April 11, 2017.

Address correspondence and reprint requests to David E. Sahar, MD, FACS, Associate Professor of Surgery, Division of Plastic Surgery, Surgical Bioengineering Laboratory, University of California—Davis Medical Center, 2221 Stockton Boulevard, Suite 2123, Sacramento, CA 95817; E-mail: dsahar@ucdavis.edu

This study was previously presented at the Military Health System Research Symposium, August 2014, Fort Lauderdale, FL and the Annual Meeting of California Society of Plastic Surgeons, May 2014, Newport Beach, CA.

This work was supported by funds from the Department of Defense Medical Research and Material Command Grant No W911QY-12-C-0141 (DES).

The authors report no conflicts of interest.

ISSN: 1049-2275
DOI: 10.1097/SCS.0000000000003910

osteoblasts and endothelial cells in an attempt to obtain a vascularized osteogenic construct. We transferred the resultant construct to critical size rat calvarial defects and evaluated bone regeneration histologically and with micro-computed tomography (CT) scans.

MATERIALS AND METHODS

All the animal experiments were approved by Institutional Animal Care and Use Committee at Travis Air Force Base, David Grant Medical Center Clinical Investigation Facility (protocol no FDG20110033A).

Harvest and Differentiation of Adipose-Derived Stem Cells

We harvested ASC from the inguinal fat pads of Lewis rats (n = 5) following the published protocols of our laboratory.[18] Briefly, inguinal fat pads were mechanically minced and digested in 0.15% collagenase solution for 45 to 60 minutes. The suspension containing digested fat was filtered through 100 μm filters (ThermoFisher Scientific, Pittsburgh, PA) and centrifuged at 1200 rpm for 5 minutes. The supernatant was discarded and the resultant cell pellet was washed with sterile phosphate-buffered saline to eliminate any contaminants. The cell pellet was plated onto 60 mm cell culture dishes (Corning, Corning, NY). Fresh medium was added to dishes twice a week and the cells were allowed to grow until 70% to 80% confluence in culture dishes before passaging. Adipose-derived stem cells between passages III and V were used for all the experiments.

We induced rat ASC toward osteoblastic lineage by feeding the cells with StemPro Osteogenesis Media (ThermoFisher Scientific) for 21 days, adding fresh medium twice a week. We confirmed osteogenic differentiation with Alizarin red staining, osteopontin (OPN) immunofluorescence (IF) staining, and qRT-PCR to detect OPN gene (the primers used for qRT-PCR are shown in Table 1). For IF staining we fixed the cells with 4% paraformaldehyde and incubated them with a primary antibody for OPN (Santa Cruz, San Diego, CA) overnight at 4°C. We used antimouse AF488 (Invitrogen, Eugene, OR) as the secondary antibody. Finally, we counterstained the nuclei with 4′,6-diamidino-2-phenylindole (Vector Laboratories, Burlingame, CA) and visualized the cells under a fluorescence microscope.

We induced rat ASC toward endothelial lineage by feeding the cells with EGM-2MV Bullet Kit (Lonza Pharmaceuticals, Basel, Switzerland) twice a week for 14 days as described previously.[12,13,19] The contents of the EGM-2MV medium are shown in Table 2. We confirmed endothelial differentiation with CD31 and von Willebrand factor (vWF) IF staining, and qRT-PCR to detect CD31 and vWF gene expression (the primers used for qRT-PCR are shown in Table 1). We used rat anti-CD31 antibody (Santa Cruz), mouse anti-vWF antibody (BD Pharmingen, San Jose, CA) as primary antibodies and antirat Texas red (Life Technologies, Carlsbad, CA), antimouse AF488 (Invitrogen) as secondary antibodies. The rest of the staining protocol was same as above.

Preparation of Hydroxyapatite/Poly (Lactide-Co-Glycolide) Scaffolds

We prepared HA-PLG scaffolds using a gas foaming/particulate leaching method as described previously.[20,21] Briefly, microspheres composed of PLG (8515 DLG 7E; Lakeshore Biomaterials, Birmingham, AL) were prepared using a double-emulsion process. Lyophilized PLG microspheres (8 mg) were mixed with 152 mg of NaCl particles (250–425 mm in diameter) and compressed to a solid disk (final dimensions: 8.5 mm diameter and 1.5 mm thickness; approximately 85 mL total volume) in a custom-made stainless steel die using a Carver press (Fred S. Carver) at 10 MPa for 1 minute. An additional 20 mg of HA nanocrystals (100 nm diameter; nm diameter; Berkeley Advanced Biomaterials, Berkeley, CA) were added to the PLG/NaCl mixture before compression to attain HA:PLG mass ratio of 2.5:1. The solid disks were exposed to high-pressure CO_2 gas (5.5 MPa) for at least 16 hours to saturate the entire disk. The pressure was rapidly (<1 min) released to ambient, causing the polymer particles to foam and ultimately fuse to create porous polymer matrices. NaCl particles were then removed from the scaffolds by leaching in distilled H_2O over 24 hours.

Cell Seeding on the Scaffolds

We seeded ASC, ASC-derived endothelial cells, and ASC-derived osteoblasts on the HA-PLG scaffolds in groups II, III, and IV, respectively (Table 3). We suspended 1×10^6 cells in 100 μL of serum-free medium and seeded the cells at a density of 5×10^3 cells/mm^2 on the scaffolds in 12-well dishes. We kept the dishes at 37°C in incubator for 2 hours to allow the cells to attach to the scaffolds. Two hours later, we added 1000 μL of cell culture media containing Dulbecco modified Eagle medium (Gibco, Grand Island, NY), 10% fetal bovine serum (Corning, Manasas, VA), 1% antibiotic–antimycotic solution (Sigma, St Louis, MO) into the wells containing scaffolds. We transplanted the scaffolds into the calvarial defects a day after cell seeding (Fig. 1).

Rat Critical Sized Calvarial Defect Model

We created 8 mm circular defects in the calvaria of male Lewis rats (n = 30) using a modification of methods described previously.[2] Briefly, we prepped and draped the heads of the animals in sterile fashion and made a 2- to 3-cm midline incision over the parietal bone using a scalpel. We incised and reflected the periosteum overlying parietal bones away using a periosteal elevator and created a circular bone defect measuring 8 mm in diameter using a drill. We paid extra caution not to disrupt the underlying dura mater that was freed from the bone using a periosteal elevator. Following adequate hemostasis, we repaired the defects using

TABLE 1. Primers Used for qRT-PCR

	Forward	Reverse
OPN	5′-AAGGCGCATTACAGCAAAACTCA-3′	5′-ATGAAGAGCCAGGAGTCCATGAG-3′
CD31	5′-TCACCAAGAGAACGGAAGGC-3′	5′-TATTTGACGGCAGCAGAGGA-3′
vWF	5′-CCGAGCCATACCTGCACATC-3′	5′-CGGATGCGCTTCTGAGAGAT-3′
GAPDH*	5′-AGACAGCCGCATTCCCTTGT-3′	5′-TGATGGCAACAATGTCAAGT-3′

OPN, osteopontin; vWF, Von Willebrand factor.
*Housekeeping gene.

TABLE 2. Contents of EGM-2MV Endothelial Differentiation Medium

EBM 2 basal medium	500 mL
Microvascular SingleQuots Kit	
VEGF	0.5 mL
Fetal bovine serum	25 mL
Hydrocortisone	0.2 mL
hFGF-B	2.0 mL
R3-IGF-1	0.5 mL
Ascorbic acid	0.5 mL
hEGF	0.5 mL
GA-1000	0.5 mL

GA-1000, gentamycin/amphotericin-B; hEGF, human epidermal growth factor hFGF-β, human fibroblast growth factor beta; R3-IGF-1, R3-insulin like growth factor-1; VEGF, vascular endothelial growth factor.

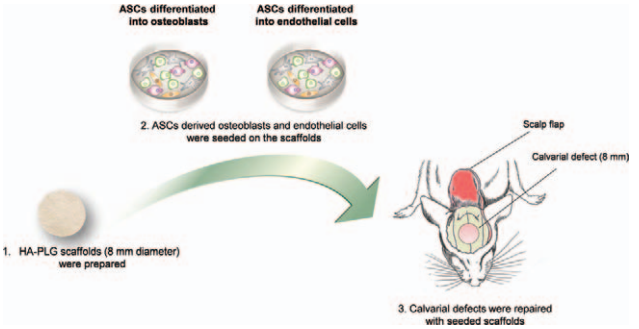

FIGURE 1. Illustration shows the experimental flow. Critical size rat calvarial defects were repaired with HA-PLG scaffolds seeded with ASC-derived osteoblasts and endothelial cells. ASC, adipose-derived stem cells; HA-PLG, hydroxyapatite/poly(lactide-co-glycolide).

corresponding methods (Fig. 1, Table 1). Lastly, we closed the skin over the repair zone using interrupted sutures with 5/0 nylon (Prolene, Ethicon US, LLC, Sommerville, NJ). Anesthesia was induced and maintained via inhalation of 2% to 5% isoflurane during animal procedures.

Evaluation of Bone Regeneration

We evaluated bone regeneration using micro-CT scans and histologic examination 8 weeks after implantation of the scaffolds. We obtained micro-CT scans under general anesthesia using a SkyScan High Resolution in vivo x-ray microtomograph (Bruker, Billerica, MA). We quantified bone mineral density (g/cm^3) on the CT images using region of interest (ROI) analysis. Briefly, we drew an 8 mm ROI on the defect zone using the SkyScan Software [CTAn(v.1.15) + CTVol(v.2.3)] and quantified the bone mineral density in the selected area. Following micro-CT scanning, we euthanized the animals and harvested their calvaria for histologic analysis. We fixed the excised calvaria including the defect zone with 4% paraformaldehyde, decalcified, embedded in paraffin blocks and cut to 5 μm sections. We stained the sections with Hematoxylin–Eosin (HE) and Masson Trichrome stain and quantified the bone tissue formed in the defect zone using ImageJ software.[22] We expressed the results as "percent of the total surface area." In addition, we calculated the vascular density in the defect zone using HE stained slides. We selected 7 slides from each group randomly and counted the number of the vessels in the whole defect zone manually under high power magnification.

Statistical Analysis

All results were compared using 1-way analysis of variance test and, if necessary, Tukey test. $P < 0.05$ was considered significant.

TABLE 3. Study Groups

Groups	n	Treatment Method
I	9	HA-PLG scaffold only
II	7	HA-PLG scaffold + ASC
III	7	HA-PLG scaffold + ASC-derived endothelial cells
IV	7	HA-PLG scaffold + ASC-derived osteoblasts

ASC, adipose-derived stem cells; HA-PLG, hydroxyapatite/poly (lactide-co-glycolide).

RESULTS

Differentiation of Adipose-Derived Stem Cells Toward Osteoblastic and Endothelial Lineages

The ASC-derived osteoblasts secreted bone matrix as detected by Alizarin red staining (Fig. 2, upper panel) and the cells stained positive for OPN in IF staining (Fig. 2, upper panel). After 3 weeks of differentiation, the expression of OPN gene also increased 6.3 ± 1.8 fold in ASC ($P < 0.05$) (Fig. 2, upper panel). The

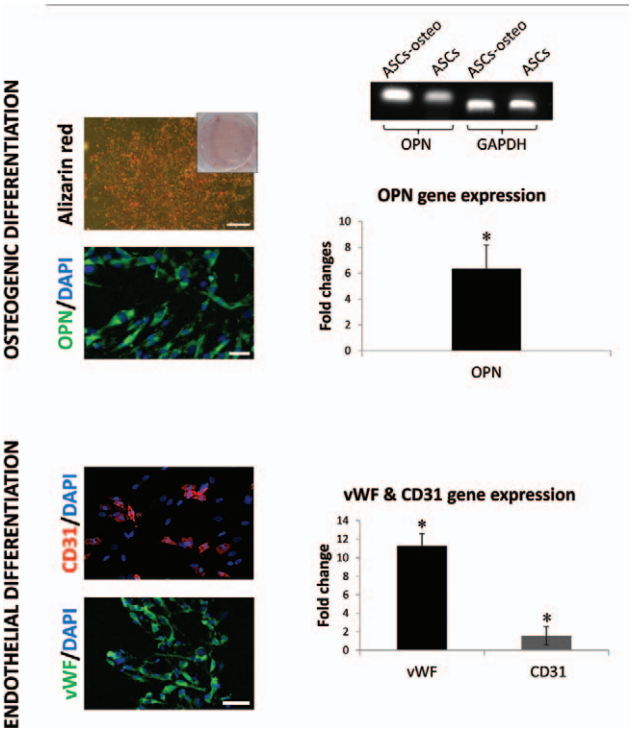

FIGURE 2. Upper panel: Alizarin red staining revealed the osteogenic matrix secreted by ASC-osteo (above left, microbar 500 μm). ASC-osteo also stained positive for OPN in IF staining (below left, microbar 50 μm) and exhibited an increase in the expression of OPN gene at the end of differentiation period compared with undifferentiated ASC (right). Lower panel: ASC-derived endothelial cells stained positive for CD31 and vWF in IF staining (above and below left, microbar 50 μm), and showed increased CD31 and vWF gene expression compared with undifferentiated ASC (right). $^*P < 0.05$. ASC, adipose-derived stem cells; ASC-osteo, ASC-derived osteoblasts; IF, immunofluorescence; OPN, osteopontin; vWF, Von Willebrand factor.

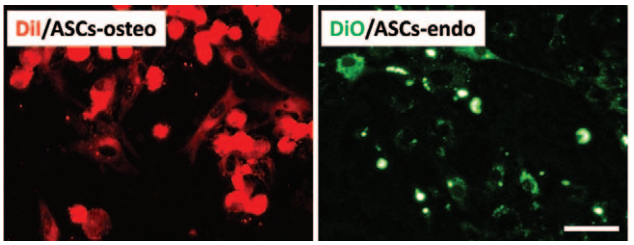

FIGURE 3. ASC-osteo (labeled with DiI) and ASC-endo (labeled with DiO) seeded on the HA-PLG scaffolds. Microbar 50 μm. ASC, adipose-derived stem cells; ASC-endo, ASC-derived endothelial cells; ASC-osteo, ASC-derived osteoblasts; HA-PLG, hydroxyapatite/poly(lactide-co-glycolide).

ASC-derived endothelial cells stained positive for CD31 and vWF (Fig. 2, lower panel). Expression of vWF and CD31 genes also increased 11.2 ± 1.3 and 1.5 ± 1.01-fold, respectively, compared with undifferentiated ASC ($P < 0.05$) (Fig. 2, lower panel). Differentiated and undifferentiated ASC both attached to the surface of HA-PLG scaffolds (Fig. 3).

Bone Regeneration

We initially included 9 animals per each group; however, 2 animals from groups II, III, and IV were excluded from the study due to postoperative complications. All the other animals survived and recovered from the surgery uneventfully.

The highest bone mineral density was in group IV [(scaffold + ASC-derived osteoblasts) (1.46 ± 0.01 g/cm^3)] followed by groups III (1.43 ± 0.05 g/cm^3), I (1.42 ± 0.05 g/cm^3), and II (1.3 ± 0.1 g/cm^3) (Fig. 4). Even though there was a trend toward increased bone regeneration in group IV in comparison to other groups, this did not achieve statistical significance ($P > 0.05$) (Fig. 4).

The results of HE and Masson Trichrome staining (Fig. 5, above) was similar to micro-CT evaluation. We observed the highest bone regeneration in group IV followed by groups II, III, and I but the difference between the groups did not achieve statistical significance ($P > 0.05$) (Fig. 5, below). Highest vascular density was in group IV but this difference also did not achieve statistical significance ($P > 0.05$) (Fig. 6).

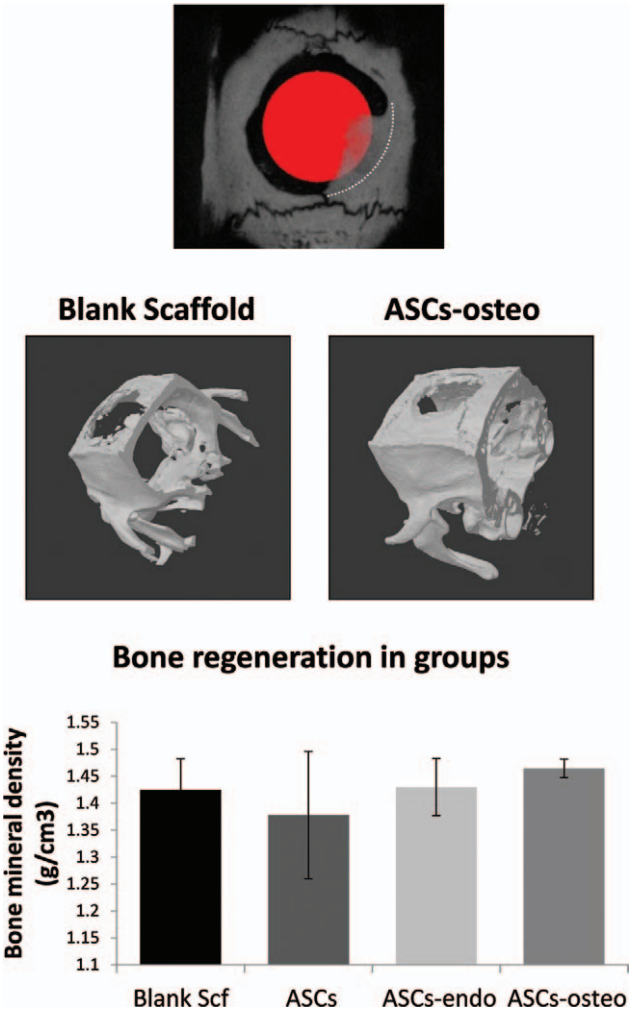

FIGURE 4. Evaluation of bone regeneration within the calvarial defect zone using region of interest (red circle) analysis (above). Micro-computed tomography scans show new bone protruding into the defect zone in ASC-osteo group, whereas there was no bone regeneration in the defects repaired with blank scaffold (middle). However, the increase in bone regeneration in ASC-osteo group was limited and bone mineral density was similar across the study groups (below). ASC, adipose-derived stem cells; ASC-endo, ASC-derived endothelial cells; ASC-osteo, ASC-derived osteoblasts.

DISCUSSION

Our beginning hypothesis in this study was that ASC-derived endothelial cells would accelerate the neovascularization of the osteogenic scaffolds and increase the bone regeneration. However, we did not observe a significant increase in bone regeneration with the use of ASC-derived endothelial cells and osteoblasts. These results are consistent with our previous report using poly lactic acid scaffolds[23] and might be explained by several possible reasons including the loss of the plasticity of ASC-derived endothelial cells after transplantation to an osteogenic environment, death of the majority of the transplanted cells (due to continuing delay in vascularization), and low seeding efficiency. We also failed to observe the well-documented angiogenic effect of ASC that might be due to the same reasons mentioned above, in particular death of the ASC after transplantation into an avascular environment, and low initial seeding efficiency.

The most striking difference between in vitro and in vivo environments is the complex 3-dimensional structure of the in vivo environment. In vitro, culture medium effectively delivers the nutrients to the cells in cell culture dishes. In contrary to this, the access of the cells to the nutrients in vivo solely relies on the neovascularization of the scaffolds following transplantation. A delay in neovascularization unquestionably leads to cell death and decreases the effectiveness of cellular treatment.[11,24] Our results suggest that seeding scaffolds with endothelial cells alone is not sufficient to stimulate neovascularization of the scaffolds. A more effective strategy might be to establish a vascular network within scaffold before transplantation so that the vascular network of the scaffolds can be anastomosed to the vessels in the recipient bed providing immediate blood flow to the scaffold. At the time of this writing, there are several research groups, including ours, working toward achieving this goal.[25,26]

An interesting finding of this study was the markedly better bone regeneration detected in the stem cell-treated groups histologically in comparison to micro-CT scans. The reason for this discrepancy might be the failure to detect immature bone tissue with micro-CT as well as the different quantification methods (ImageJ vs SkyScan Software). Since histologic analysis is a more direct method of evaluation, we believe that our histologic results reflect the extend of bone regeneration in cell treatment groups better than micro-CT scans. There is a visibly stronger trend toward better bone

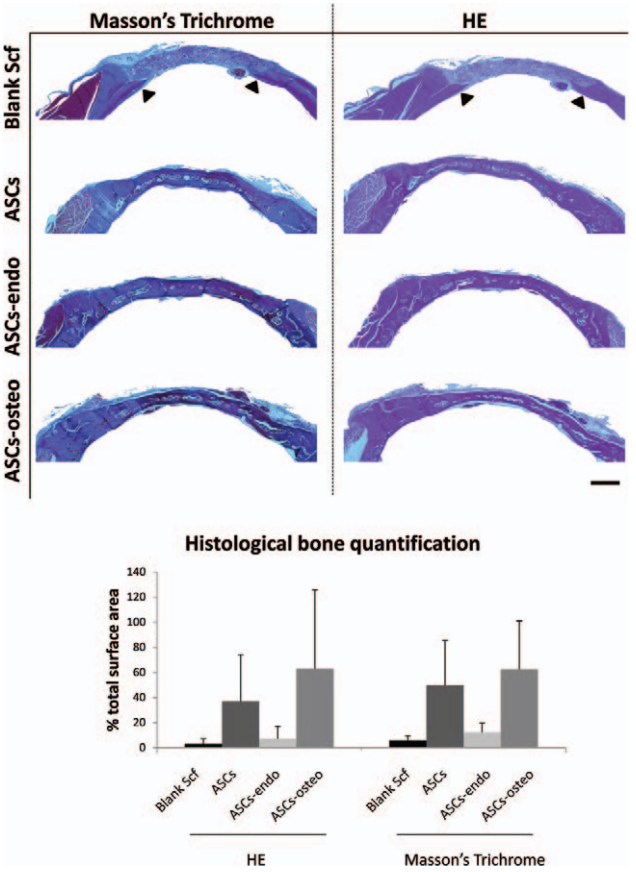

FIGURE 5. Hematoxylin–Eosin and Masson Trichrome staining for histologic evaluation of bone regeneration (above, microbar 500 μm). Black arrow heads mark the border between the intact calvarial bone and the scaffold occupying the defect. Even though representative pictures show better bone regeneration in cell treated groups (II, III, IV) in comparison to defects treated with only blank scaffold (group I), percent regenerated bone area within the whole defect zone was similar across the groups (below). ASC, adipose-derived stem cells; ASC-endo, ASC-derived endothelial cells; ASC-osteo, ASC-derived osteoblasts.

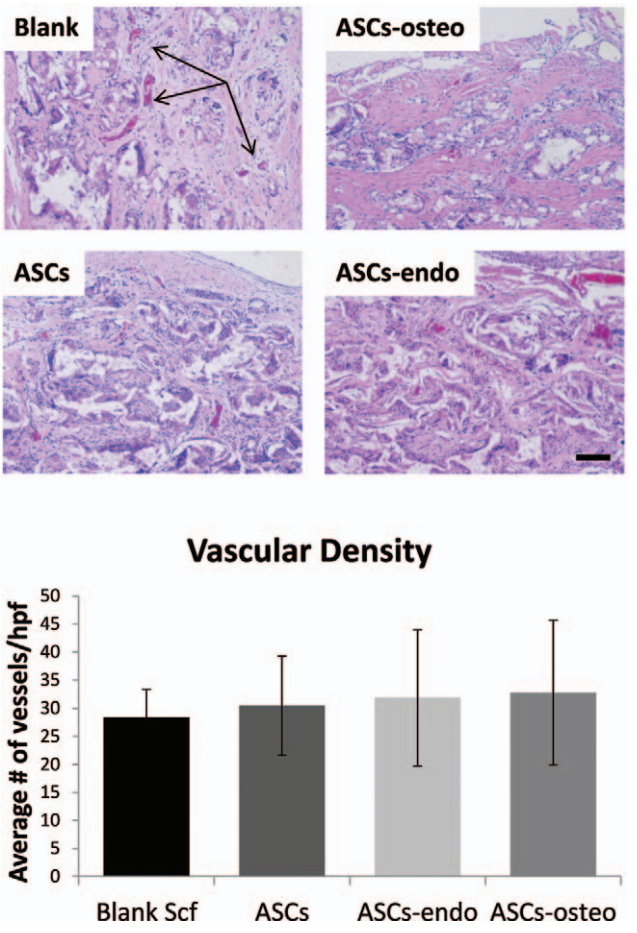

FIGURE 6. Vascular density in the defect zone was also similar across the groups as seen in Hematoxylin–Eosin stained slides ($P < 0.05$). Black arrows mark the vessels. Microbar 100 μm. ASC, adipose-derived stem cells; ASC-endo, ASC-derived endothelial cells; ASC-osteo, ASC-derived osteoblasts.

regeneration in cell-treated groups in histologic slides, only masked by wide standard deviation bars. Decreasing the deviation within the groups by increasing the sample size might conceive the real osteogenic potential of ASCs and ASCs-derived endothelial cells and osteoblasts.

Despite the controversial reports on their osteogenic potential, ASC are safe and can function as a continuous source of growth factors in vivo,[16,24,27] and still hold the potential to become a valuable tool in bone tissue engineering. Several other strategies for bone regeneration have been described in the literature; bone morphogenetic protein-2 (BMP-2),[28] recombinant angiogenic proteins,[6,29] and proangiogenic materials[7,27] were all shown to induce angiogenesis, and osteogenesis when used in conjunction with osteogenic scaffolds. Moreover, BMP-2 was found superior to ASC in terms of stimulation of bone regeneration.[28] However, it should be noted that these molecules are quickly degraded in vivo, hence have a short-lasting effect, and potentially serious side effects at clinical doses.[30–33] The ideal solution might be using a combination of these tools instead of using them as opposite alternatives. Such a combination may have synergistic effects on bone healing and allow us to avoid the side effects of singular treatments in clinical application by decreasing the required doses.[29,34]

Another point that merits discussion is the ideal stem cell type for bone tissue engineering. We opt to use ASC in this study considering the ease of access and harvest; however, bone marrow-derived stem cells are known to have a higher osteogenic potential than ASC,[35] and may have yielded a better bone regeneration in our animal model. The pros and cons of these stem cell types should be weighed against each other carefully, preferably on a case-by-case basis, in clinical application.

Despite the major roadblocks to efficient clinical application, the number of tissue engineering methods for calvarial bone reconstruction has increased steeply in recent years. Developments in 3-dimensional printing, tissue engineering, and osteoinductive delivery systems allowed the development of computer-designed implants, which can be tailored to the shape of complex craniofacial defects.[4] Some of these new technologies have been tested in the clinic on a limited number of patients and yielded favorable results encouraging future studies.[24,36–41] However, as suggested by our results, vascularity remains to be an obstacle in tissue engineering. Refinement of the cell delivery vehicles (ie, scaffolds) and development of new strategies to induce angiogenesis and neovascularization are mandatory to accelerate the clinical translation of bone tissue engineering methods.

In conclusion, ASC-derived endothelial cells and osteoblasts seeded on HA-PLG scaffolds provided a limited increase in vascularization and bone regeneration compared with scaffolds alone. Detailed studies are needed to determine the exact reason(s) for these results and possible solutions.

ACKNOWLEDGMENT

The authors thank Sarah A. StClaire for her technical assistance with the illustrations.

REFERENCES

1. Perry CR. Bone repair techniques, bone graft, and bone graft substitutes. *Clin Orthop Relat Res* 1999;360:71–86
2. Gomes PS, Fernandes MH. Rodent models in bone-related research: the relevance of calvarial defects in the assessment of bone regeneration strategies. *Lab Anim* 2011;45:14–24
3. Oppenheimer AJ, Mesa J, Buchman SR. Current and emerging basic science concepts in bone biology: implications in craniofacial surgery. *J Craniofac Surg* 2012;23:30–36
4. Chim H, Schantz JT. New frontiers in calvarial reconstruction: integrating computer-assisted design and tissue engineering in cranioplasty. *Plast Reconstr Surg* 2005;116:1726–1741
5. Giannoudis PV, Pountos I. Tissue regeneration. The past, the present and the future. *Injury* 2005;36(suppl 4):S2–S5
6. Leach JK, Kaigler D, Wang Z, et al. Coating of VEGF-releasing scaffolds with bioactive glass for angiogenesis and bone regeneration. *Biomaterials* 2006;27:3249–3255
7. Leu A, Stieger SM, Dayton P, et al. Angiogenic response to bioactive glass promotes bone healing in an irradiated calvarial defect. *Tissue Eng Part A* 2009;15:877–885
8. Kaigler D, Wang Z, Horger K, et al. VEGF scaffolds enhance angiogenesis and bone regeneration in irradiated osseous defects. *J Bone Miner Res* 2006;21:735–744
9. Murphy KC, Stilhano RS, Mitra D, et al. Hydrogel biophysical properties instruct coculture-mediated osteogenic potential. *FASEB J* 2016;30:477–486
10. Unger RE, Ghanaati S, Orth C, et al. The rapid anastomosis between prevascularized networks on silk fibroin scaffolds generated in vitro with cocultures of human microvascular endothelial and osteoblast cells and the host vasculature. *Biomaterials* 2010;31:6959–6967
11. Jain RK, Au P, Tam J, et al. Engineering vascularized tissue. *Nat Biotechnol* 2005;23:821–823
12. Planat-Benard V, Silvestre JS, Cousin B, et al. Plasticity of human adipose lineage cells toward endothelial cells: physiological and therapeutic perspectives. *Circulation* 2004;109:656–663
13. Cao Y, Sun Z, Liao L, et al. Human adipose tissue-derived stem cells differentiate into endothelial cells in vitro and improve postnatal neovascularization in vivo. *Biochem Biophys Res Commun* 2005;332:370–379
14. Cheung WK, Working DM, Galuppo LD, et al. Osteogenic comparison of expanded and uncultured adipose stromal cells. *Cytotherapy* 2010;12:554–562
15. Haynesworth SE, Baber MA, Caplan AI. Cytokine expression by human marrow-derived mesenchymal progenitor cells in vitro: effects of dexamethasone and IL-1 alpha. *J Cell Physiol* 1996;166:585–592
16. Caplan AI, Dennis JE. Mesenchymal stem cells as trophic mediators. *J Cell Biochem* 2006;98:1076–1084
17. Gimble JM, Katz AJ, Bunnell BA. Adipose-derived stem cells for regenerative medicine. *Circ Res* 2007;100:1249–1260
18. Orbay H, Little CJ, Lankford L, et al. The key components of Schwann cell-like differentiation medium and their effects on gene expression pattern of adipose-derived stem cells. *Ann Plast Surg* 2015;74:584–588
19. Colazzo F, Chester AH, Taylor PM, et al. Induction of mesenchymal to endothelial transformation of adipose-derived stem cells. *J Heart Valve Dis* 2010;19:736–744
20. Li D, Ye C, Zhu Y, et al. Fabrication of poly(lactide-co-glycolide) scaffold embedded spatially with hydroxyapatite particles on pore walls for bone tissue engineering. *Polymers Adv Technol* 2012;23:1446–1453
21. He J, Genetos DC, Leach JK. Osteogenesis and trophic factor secretion are influenced by the composition of hydroxyapatite/poly(lactide-co-glycolide) composite scaffolds. *Tissue Eng Part A* 2010;16:127–137
22. Schneider CA, Rasband WS, Eliceiri KW. NIH Image to ImageJ: 25 years of image analysis. *Nat Methods* 2012;9:671–675
23. Sahar DE, Walker JA, Wang HT, et al. Effect of endothelial differentiated adipose-derived stem cells on vascularity and osteogenesis in poly(D,L-lactide) scaffolds in vivo. *J Craniofac Surg* 2012;23:913–918
24. Rajan A, Eubanks E, Edwards S, et al. Optimized cell survival and seeding efficiency for craniofacial tissue engineering using clinical stem cell therapy. *Stem Cells Transl Med* 2014;3:1495–1503
25. Chang EI, Bonillas RG, El-Ftesi S, et al. Tissue engineering using autologous microcirculatory beds as vascularized bioscaffolds. *FASEB J* 2009;23:906–915
26. Jacoby A, Morrison KA, Hooper RC, et al. Fabrication of capillary-like structures with Pluronic F127(R) and *Kerria lacca* resin (shellac) in biocompatible tissue-engineered constructs. *J Tissue Eng Regen Med* 2017;11:2388–2397
27. He J, Decaris ML, Leach JK. Bioceramic-mediated trophic factor secretion by mesenchymal stem cells enhances in vitro endothelial cell persistence and in vivo angiogenesis. *Tissue Eng Part A* 2012;18:1520–1528
28. Smith DM, Cooper GM, Afifi AM, et al. Regenerative surgery in cranioplasty revisited: the role of adipose-derived stem cells and BMP-2. *Plast Reconstr Surg* 2011;128:1053–1060
29. Huang YC, Kaigler D, Rice KG, et al. Combined angiogenic and osteogenic factor delivery enhances bone marrow stromal cell-driven bone regeneration. *J Bone Miner Res* 2005;20:848–857
30. Cooper GS, Kou TD. Risk of cancer after lumbar fusion surgery with recombinant human bone morphogenic protein-2 (rh-BMP-2). *Spine (Phila Pa 1976)* 2013;38:1862–1868
31. Merrick MT, Hamilton KD, Russo SS. Acute epidural lipedema: a novel entity and potential complication of bone morphogenetic protein use in lumbar spine fusion. *Spine J* 2013;13:e15–e19
32. Fisher DM, Wong JM, Crowley C, et al. Preclinical and clinical studies on the use of growth factors for bone repair: a systematic review. *Curr Stem Cell Res Ther* 2013;8:260–268
33. Moeinzadeh S, Jabbari E. Morphogenic peptides in regeneration of load bearing tissues. *Adv Exp Med Biol* 2015;881:95–110
34. Fan J, Im CS, Guo M, et al. Enhanced osteogenesis of adipose-derived stem cells by regulating bone morphogenetic protein signaling antagonists and agonists. *Stem Cells Transl Med* 2016;5:539–551
35. Li CY, Wu XY, Tong JB, et al. Comparative analysis of human mesenchymal stem cells from bone marrow and adipose tissue under xeno-free conditions for cell therapy. *Stem Cell Res Ther* 2015;6:55
36. Behnia H, Khojasteh A, Soleimani M, et al. Repair of alveolar cleft defect with mesenchymal stem cells and platelet derived growth factors: a preliminary report. *J Craniomaxillofac Surg* 2012;40:2–7
37. Gan Y, Dai K, Zhang P, et al. The clinical use of enriched bone marrow stem cells combined with porous beta-tricalcium phosphate in posterior spinal fusion. *Biomaterials* 2008;29:3973–3982
38. Kaigler D, Avila-Ortiz G, Travan S, et al. Bone engineering of maxillary sinus bone deficiencies using enriched CD90+ stem cell therapy: a randomized clinical trial. *J Bone Miner Res* 2015;30:1206–1216
39. Kaigler D, Pagni G, Park CH, et al. Stem cell therapy for craniofacial bone regeneration: a randomized, controlled feasibility trial. *Cell Transplant* 2013;22:767–777
40. Marcacci M, Kon E, Moukhachev V, et al. Stem cells associated with macroporous bioceramics for long bone repair: 6- to 7-year outcome of a pilot clinical study. *Tissue Eng* 2007;13:947–955
41. Sauerbier S, Rickert D, Gutwald R, et al. Bone marrow concentrate and bovine bone mineral for sinus floor augmentation: a controlled, randomized, single-blinded clinical and histological trial—per-protocol analysis. *Tissue Eng Part A* 2011;17:2187–2197